Utah State University
DigitalCommons@USU

All Physics Faculty Publications | Physics

6-1995

Finite Thermal Diffusivity at Onset of Convection in Autocatalytic Systems: Discontinuous Fluid Density

D. A. Vasquez

Boyd F. Edwards
Utah State University

J. W. Wilder

Follow this and additional works at: http://digitalcommons.usu.edu/physics_facpub

Part of the Physics Commons

Recommended Citation
"Finite thermal diffusivity at onset of convection in autocatalytic systems: Discontinuous fluid density," D. A. Vasquez, B. F. Edwards, and J. W. Wilder, Phys. Fluids 7, 2513 (1995) [8].

This Article is brought to you for free and open access by the Physics at DigitalCommons@USU. It has been accepted for inclusion in All Physics Faculty Publications by an authorized administrator of DigitalCommons@USU. For more information, please contact becky.thoms@usu.edu.

UtahStateUniversity
MERRILL-CAZIER LIBRARY

Finite thermal diffusivity at onset of convection in autocatalytic systems: Discontinuous fluid density

Desiderio A. Vasquez
Department of Physics, Indiana University–Purdue University Fort Wayne, Fort Wayne, Indiana 46805-1499

Boyd F. Edwards
Department of Physics, West Virginia University, P.O. Box 6315, Morgantown, West Virginia 26506-6315

Joseph W. Wilder
Department of Mathematics, West Virginia University, P.O. Box 6310, Morgantown, West Virginia 26506-6310

(Received 22 October 1993; accepted 21 June 1995)

A linear convective stability analysis for propagating autocatalytic reaction fronts includes density differences due to both thermal and chemical gradients. Critical parameters for the onset of convection are calculated for an unbounded geometry, a vertical slab, and a vertical cylinder. Thermal effects are important at unstable wavelengths well above the critical wavelength for the onset of convection. © *1995 American Institute of Physics.*

Experiments observe convection for ascending iodate-arsenous acid fronts in vertical tubes whose diameters exceed a critical diameter of about 1 mm.[1,2] Linear hydrodynamic stability theory[3,4] predicts a transition to buoyancy-driven convection with a critical diameter that agrees with these experiments, although large experimental and theoretical uncertainties preclude a precise comparison. A 24% theoretical uncertainty is due to the difference between the critical diameters calculated for infinite and zero thermal diffusivity. To reduce this uncertainty, calculations are needed at finite thermal diffusivity.

The equation of state $\rho(T) = \rho_1\gamma[1 - \alpha(T - T_1)]$ is a first-order Taylor expansion of the temperature-dependent mass density about T_1, the final adiabatic temperature of the reacted fluid. Here, $\gamma=1$ in the unreacted fluid and $\gamma=1-\delta_1$ in the reacted fluid to account for chemically driven density changes, and α is the isobaric thermal expansion coefficient.

Neglecting small density changes $\delta_1\approx\alpha\Delta T\approx 1\times 10^{-4}$ except where they modify gravity to first order allows us to write the dimensionless thermohydrodynamic equations of motion as

$$\frac{\partial \mathbf{v}}{\partial t}+(\mathbf{v}\cdot\nabla)\mathbf{v}=-\mathscr{S}\mathscr{D}_C(T_1-T)\hat{z}-\nabla P+\nabla^2\mathbf{v}, \tag{1a}$$

$$\nabla\cdot\mathbf{v}=0, \tag{1b}$$

and

$$\frac{\partial T}{\partial t}+\mathbf{v}\cdot\nabla T=\mathscr{D}_T\nabla^2 T. \tag{1c}$$

These are measured in units of length a to be specified below, time a^2/ν, pressure $\rho_1\nu^2/a^2$, and temperature δ_1/α, where ν is the kinematic viscosity. The convenient reduced pressure P is related to the conventional pressure by $P=P_{\text{conv}}+(\gamma g a^3/\nu^2)z$. The equations also involve a dimensionless thermal diffusivity $\mathscr{D}_T=D_T/\nu$, a dimensionless molecular diffusivity $\mathscr{D}_C=D_C/\nu$, and a dimensionless driving parameter $\mathscr{S}=\delta_1 a^3 g/\nu D_C$.

The location of the thin chemical front is given by $z=h(x,y,t)$, a function of the horizontal coordinates and the time, obeying the eikonal relation[3]

$$\hat{\mathrm{n}}\cdot\hat{\mathrm{z}}\frac{\partial h}{\partial t}=v_0+\mathscr{D}_C\kappa+\hat{\mathrm{n}}\cdot\mathbf{v}|_h. \tag{1d}$$

Here, $\hat{\mathrm{n}}$ is the normal vector to the front pointing into the unreacted fluid, $v_0=(a/\nu)c_0$ is the dimensionless flat front speed, $\mathbf{v}|_h$ is the fluid velocity evaluated at $z=h(x,y,t)$, and κ is the curvature of the front measured as positive when the center of curvature is in the unreacted fluid.

The boundary conditions require that the velocity and the normal derivative of the temperature vanish at the sidewalls, ensuring no-slip, insulating sidewalls. The jump conditions at the front[3] express the conservation of energy, mass and momentum:

$$[\hat{\mathrm{n}}\cdot\mathbf{v}]_h=0, \tag{1e}$$

$$[\hat{\mathrm{n}}\times\mathbf{v}]_h=0, \tag{1f}$$

$$[\epsilon_{ijk}n_j n_l T^v_{kl}]_h=0, \tag{1g}$$

$$[P]_h=-\mathscr{S}\mathscr{D}_C h-[n_i n_j T^v_{ij}]_h, \tag{1h}$$

$$[\hat{\mathrm{n}}\cdot\nabla T]_h=\frac{\Delta T}{\mathscr{D}_T}\left(\hat{\mathrm{n}}\cdot\hat{\mathrm{z}}\frac{\partial h}{\partial t}-\hat{\mathrm{n}}\cdot\mathbf{v}|_h\right), \tag{1i}$$

and

$$[T]_h=0. \tag{1j}$$

Here, $[q]_h$ denotes the jump in a given function $q=q(\mathbf{x},t)$ in the following way. If $q(\mathbf{x},t)=q_r(\mathbf{x},t)$ in the reacted fluid and $q(\mathbf{x},t)=q_u(\mathbf{x},t)$ in the unreacted fluid, then $[q]_h\equiv q_r|_h-q_u|_h$ is the difference between these functions evaluated at the reaction front $z=h$. Furthermore, $T^v_{ij}=-\partial v_i/\partial x_j-\partial v_j/\partial x_i$ is the (dimensionless) viscous stress tensor, ϵ_{ijk} is the totally antisymmetric tensor, n_i are the Cartesian components of $\hat{\mathrm{n}}$, and $\Delta T=T_1-T_0$ involves the initial fluid temperature T_0. Equations (1) determine the convective motion and stability of a thin autocatalytic reaction front.

Steady upward propagation of a convectionless flat front is conveniently described in a frame of reference that is stationary with respect to the front. With the front located at

Downloaded 11 Oct 2011 to 129.123.124.160. Redistribution subject to AIP license or copyright; see http://pof.aip.org/about/rights_and_permissions

$z=h^{(0)}=0$ (and the unreacted fluid at $z>h^{(0)}$), Eqs. (1) give $\mathbf{v}^{(0)}=-v_0\hat{\mathbf{z}}$, $\hat{\mathbf{n}}^{(0)}=\hat{\mathbf{z}}$, $h^{(0)}=\kappa^{(0)}=0$, $\partial P^{(0)}/\partial z=\mathscr{S}\mathscr{D}_C\gamma \times (T^{(0)}-T_1)$, as well as temperatures

$$T_r^{(0)}=T_1 \tag{2a}$$

and

$$T_u^{(0)}=T_0+\Delta T e^{-zv_0/\mathscr{D}_T} \tag{2b}$$

in the reacted and unreacted fluids. This solution lacks both fluid motion (in the laboratory frame) and horizontal thermal gradients. Hence, it is applicable to both unbounded geometries and geometries with vertical insulating sidewalls.

To study the stability of the convectionless flat front, we perturb it slightly according to $\mathbf{v}=\mathbf{v}^{(0)}+\mathbf{v}^{(1)}$, with similar forms for the other dependent variables. In evaluating Eqs. (1) for small h, it is convenient to employ Taylor expansions,

$$q|_h=q|_0+h\partial_z q|_0+\tfrac{1}{2}h^2\partial_z^2 q|_0+\cdots \tag{3a}$$

and

$$[q]_h=[q]_0+h[\partial_z q]_0+\tfrac{1}{2}h^2[\partial_z^2 q]_0+\cdots, \tag{3b}$$

where $\partial_z=\partial/\partial z$. Note that even though $q(\mathbf{x},t)=q_u(\mathbf{x},t)$ only for $z>h(x,y,t)$ and $q(\mathbf{x},t)=q_r(\mathbf{x},t)$ only for $z<h(x,y,t)$, the functions $q_r(\mathbf{x},t)$ and $q_u(\mathbf{x},t)$ are defined over all space, so that the difference $[q]_0=q_r|_0-q_u|_0$ between these functions at $z=0$ is a well-defined quantity. Using these in Eqs. (1) and linearizing in the perturbations yields

$$(\partial_t-v_0\partial_z-\nabla^2)\,\mathbf{v}^{(1)}=\mathscr{S}\mathscr{D}_C T^{(1)}\hat{\mathbf{z}}-\nabla P^{(1)}, \tag{4a}$$

$$(\partial_t-v_0\partial_z-\mathscr{D}_T\nabla^2)T^{(1)}+(\partial_z T^{(0)})w^{(1)}=0, \tag{4b}$$

$$\nabla\cdot\mathbf{v}^{(1)}=0, \tag{4c}$$

$$(\partial_t-\mathscr{D}_C\nabla^2)h^{(1)}=w^{(1)}|_0, \tag{4d}$$

$$[w^{(1)}]_0=0, \tag{4e}$$

$$[\hat{\mathbf{z}}\times\mathbf{v}^{(1)}]_0=0, \tag{4f}$$

$$[\epsilon_{i3k}T^{v}_{k3}{}^{(1)}]_0=0, \tag{4g}$$

$$[P^{(1)}]_0=-\mathscr{S}\mathscr{D}_C h^{(1)}+2[\partial_z w^{(1)}]_0, \tag{4h}$$

$$[T^{(1)}]_0=-\frac{\Delta T v_0}{\mathscr{D}_T}h^{(1)}, \tag{4i}$$

and

$$[\partial_z T^{(1)}]_0=\frac{\Delta T}{\mathscr{D}_T}\left(\frac{v_0^2}{\mathscr{D}_T}+\mathscr{D}_C\nabla^2\right)h^{(1)}. \tag{4j}$$

Here, we have appropriately set $\hat{\mathbf{n}}^{(1)}=-\nabla h^{(1)}$ (a horizontal vector) and $\kappa^{(1)}=\nabla^2 h^{(1)}$, and have written the vertical velocity as $w^{(1)}=\hat{\mathbf{z}}\cdot\mathbf{v}^{(1)}$.

The unbounded system is the simplest possible geometry in which to study convection in autocatalytic systems. Here we analyze the time dependence of infinitesimal perturbations about a convectionless flat unbounded front. For simplicity, we analyze two-dimensional perturbations $\mathbf{v}^{(1)}(x,z,t)=u^{(1)}(x,z,t)\hat{\mathbf{x}}+w^{(1)}(x,z,t)\hat{\mathbf{z}}$ by assigning the exponential dependence $e^{iqx+\sigma t}$ to all perturbed quantities. Substituting these forms into Eqs. (4) yields a system of ordinary differential equations that is similar to Eqs. (9) in Ref. 5, except for an important contribution from the discontinuous density. Exponential solutions are readily obtained after the manner of Ref. 5.

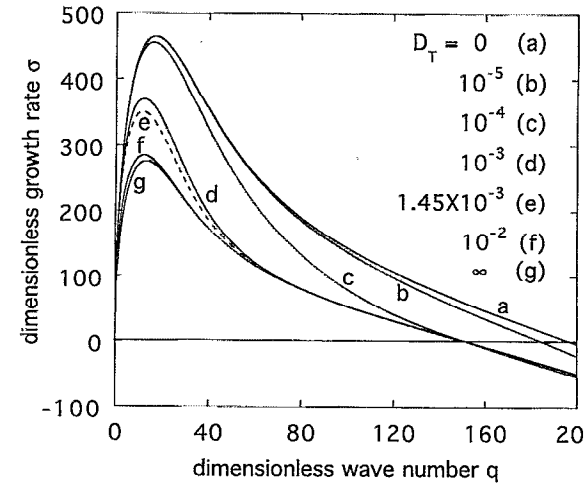

FIG. 1. Dimensionless growth rate σ for two-dimensional perturbations of dimensionless wave number q about a flat ascending reaction front in a laterally unbounded geometry for various thermal diffusivities D_T measured in units of cm^2/s, with the dashed trace corresponding to the thermal diffusivity of water.

Figure 1 shows the resulting growth rate σ of infinitesimal perturbations about a flat front as a function of the wave number q for the typical parameters[3] $D_C=2\times10^{-5}$ cm^2/s, $\delta_1=0.87\times10^{-4}$, $\Delta T=0.4°C$, $\nu=9.2\times10^{-3}$ cm^2/s, and $c_0=2.95\times10^{-3}$ cm/s for various values of the thermal diffusivity D_T, where the results for $D_T=0$ (trace a) and $D_T=\infty$ (trace g) are taken from Ref. 3. For the experimental value $D_T=1.45\times10^{-3}$ cm^2/s (trace e), the cutoff wavenumber $q_c=152$ where $\sigma=0$ agrees very well with the infinite D_T result (trace g), indicating an effectively infinite thermal diffusivity. This result can also be seen in Fig. 2. In contrast, the maximum dimensionless growth rate σ_m and the corresponding wave number q_m for this value of D_T (trace e) differ significantly from their infinite diffusivity limits. For $q\to0$ and this same value of D_T, the growth rate agrees with the $D_T=0$ limit (trace a). Figure 2 emphasizes that q_c crosses over from effectively zero to effectively infinite thermal diffusivity at a lower value of D_T than q_m and σ_m.

To understand the crossover from zero to infinite thermal diffusivity, we need only compare the convective length scale with the thermal length scale. The thermal length scale $d_T=D_T/c_0$ in conventional units [see Eq. (4b)] gives the vertical distance over which the temperature falls from T_1 to T_0. The convective length scale $d=(\nu/c_0)2\pi/q$ in conventional units is set by the dimensionless horizontal wave number q, and gives the vertical extent over which the fluid participates in the convection. In the infinite thermal diffusivity limit $d<<d_T$, the fluid participating in the convection is all essentially at the reacted fluid temperature T_1, and the fluid is unable to take advantage of the thermally induced density changes which are well above the convective region. On the other hand, in the zero thermal diffusivity limit

Downloaded 11 Oct 2011 to 129.123.124.160. Redistribution subject to AIP license or copyright; see http://pof.aip.org/about/rights_and_permissions

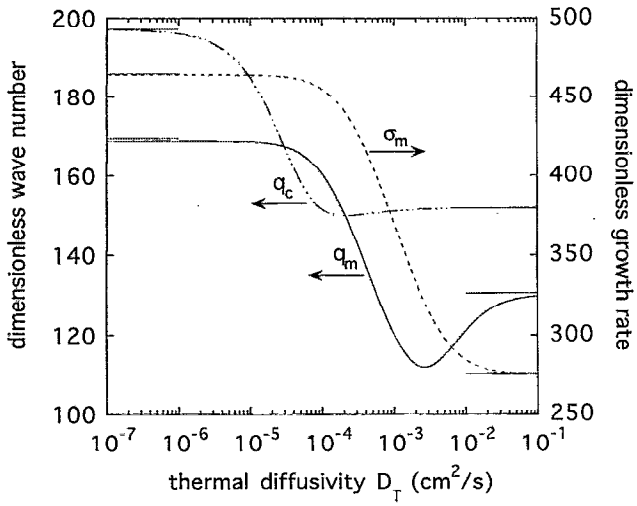

FIG. 2. Maximum dimensionless growth rate σ_m (dashed trace) and its corresponding dimensionless wave number q_m (solid trace), along with the cutoff dimensionless wave number q_c (chain-dashed trace) of zero growth rate, all as a function of the thermal diffusivity D_T. Horizontal line segments give previous asymptotic results for large and small diffusivities.[3]

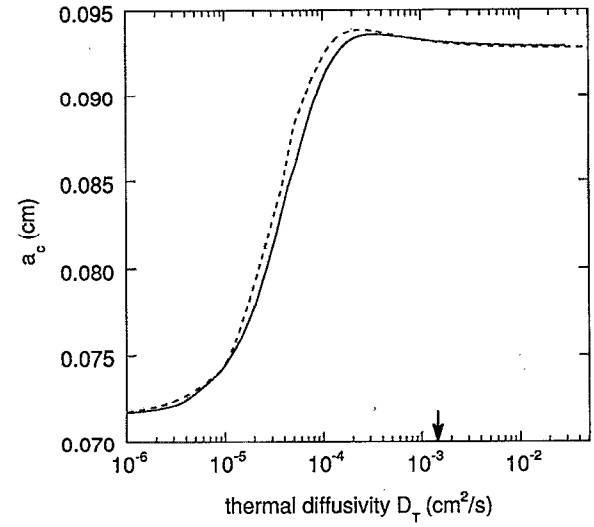

FIG. 3. Critical wall separation a_c (solid trace) and tube diameter a_c (dashed trace) vs. thermal diffusivity D_T. The vertical arrow marks the experimental thermal diffusivity $D_T = 1.45\times 10^{-3}$ cm²/s.

$d >> d_T$, the thermally induced density changes occur over a region small compared with the convective region, which extends well into the unreacted fluid at temperature T_0. The crossover between zero and infinite diffusivity should therefore occur when $d \approx d_T$, that is, when $D_T^{\text{cross}} \approx 2\pi\nu/q$. Since the values $11 < q_m < 17$ of q_m are much smaller than the values $150 < q_c < 200$ of q_c over the whole range of D_T (Fig. 2), the crossover value $D_T^{\text{cross}} \approx 4\times 10^{-3}$ cm²/s for q_m must exceed the crossover value $D_T^{\text{cross}} \approx 3\times 10^{-4}$ cm²/s for q_c. Indeed, these crossover values are consistent with the crossover behavior in Fig. 2.

Intriguing minima in q_c and q_m occur in Fig. 2 near the crossover values of D_T, where the convective and thermal length scales are comparable. At the minimum in q_c, the flat front is most stable to convective perturbations, and is even more stable than for infinite thermal diffusivity. This is due to thermal stabilization of the perturbed front: Because heat flow is normal to the front surface [Eq. (1i)], the unreacted fluid above the valleys in the front is heated faster than the fluid above the peaks. Thermal expansion consequently renders the fluid above the valleys more buoyant than otherwise, thus tending to raise the valleys and lower the peaks. This stabilizing mechanism is absent at infinite thermal diffusivity where the fluid temperature is effectively uniform throughout. It is also absent at zero thermal diffusivity, where all thermal gradients are confined to the front surface itself. Thermal stabilization is only relevant when the convective and thermal length scales are comparable, where it produces the minima in q_c and q_m.

The two-dimensional motion of a fluid confined between two parallel vertical planes located at $x = \pm a/2$ and the axisymmetric motion of a fluid confined to the interior of a long vertical cylinder of radius a are studied by generalizing the expansion procedure in Ref. 4. In each case, a flat ascending front is linearly unstable to convection above a critical length scale a_c for the onset of convection (Fig. 3). The limits of zero and infinite thermal diffusivity agree with our previous calculations.[4] The maximum in a_c implies maximum stability, and corresponds to the minimum in q_c discussed earlier. Results for $D_T = 1.45\times 10^{-3}$ cm²/s (vertical arrow), can clearly be approximated by the infinite diffusivity limit.

In conclusion, chemical gradients overwhelm thermal gradients in determining the length scale for the onset of convection in autocatalytic reaction fronts. However, at larger convective length scales approaching the thermal length scale, thermal gradients are important. An additional mechanism for stabilizing ascending reaction fronts, relevant only at finite thermal diffusivity, arises from the enhanced (depressed) heating rates above valleys (peaks) in the front, which renders the fluid above the valleys hotter and more buoyant than otherwise. This mechanism may play a crucial role in systems for which chemical and thermal gradients compete rather than cooperate with each other to destabilize the system.

ACKNOWLEDGMENTS

Discussions with Kenneth Showalter and support from National Science Foundation Grants No. RII-8922106 and No. OSR-9255224 and the National Research Center for Coal and Energy are gratefully acknowledged.

[1]T. McManus, "Chemical waves in the iodate-arsenous acid reaction," Ph.D. thesis, West Virginia University, 1989, Chap. 3.

[2]J. A. Pojman, I. R. Epstein, T. J. McManus, and K. Showalter, "Convective effects on chemical waves. 2. Simple convection in the iodate-arsenous acid system," J. Phys. Chem. **95**, 1299 (1991).

[3]B. F. Edwards, J. W. Wilder, and K. Showalter, "Onset of convection for autocatalytic reaction fronts: Laterally unbounded systems," Phys. Rev. A **43**, 749 (1991).

[4]D. A. Vasquez, B. F. Edwards, and J. W. Wilder, "Onset of convection for autocatalytic reaction fronts: Laterally bounded systems," Phys. Rev. A **43**, 6694 (1991).

[5]J. W. Wilder, B. F. Edwards, and D. A. Vasquez, "Finite thermal diffusivity at onset of convection in autocatalytic systems: Continuous fluid density," Phys. Rev A **45**, 2320 (1992).

Downloaded 11 Oct 2011 to 129.123.124.160. Redistribution subject to AIP license or copyright; see http://pof.aip.org/about/rights_and_permissions